Quantum-Chemical Studies of Fluoroethanes: Vibrational Assignments, Isolated CH Stretching Frequencies, Valence Force Constants, and Bond Length Relationships

Donald C. McKean

Department of Chemistry, University of Edinburgh, West Mains Road, Edinburgh EH9 3JJ, U.K.

Received: April 26, 2000; In Final Form: July 12, 2000

Harmonic force fields for the series of fluoroethanes, derived from HF and B3LYP calculations with the 6-311G** basis set, are scaled individually for each molecule and for each type of CH bond. Reassignments are made in the νCH region with the aid of earlier correlations between CH bond length and six observed isolated CH stretching frequencies ν^{is}CH. Eleven more ν^{is}CH values are obtained from the spectra through the determination of scale factors. Estimation of the remaining three undetermined ν^{is}CH values is discussed. Problems of assignment remain both in the νCH region and also between 1200 and 1000 cm^{-1}, which call for further study. Improved predictions are made of unobserved frequencies in the less abundant conformers of the 1,2-, 1,1,2-, and 1,1,2,2- fluoroethanes. νCH scale factors vary significantly according to the number of fluorine atoms attached to the same carbon and also to a lesser degree among those of the same type. Scale factors for other types of motion also vary both between molecules and also within a given molecule. Changes in the factor for torsional motion are particularly large. For the CH, CF, and CC bonds, unscaled valence force constants are given, and their relation to ν^{is}CH, bond lengths, and bond length "offset" values is discussed. Evidence for variations in the latter is reviewed. An unscaled ν^{is}CH value reflects very closely the corresponding CH stretching force constant in any of the groups methyl, methylene, and methine.

Introduction

The environmental interest in the properties of hydrofluorocarbons has prompted a number of recent studies of the vibrational properties of fluoroethanes, experimentally,[1−11] by the ab initio approach [12−18] or by both methods. [19−22] These have led to improvements in the assignment of observed vibration frequencies and to better predictions of those which remain as yet unobserved. However, that part of each spectrum that contains bands derived from CH stretching motions is in many instances still imperfectly understood, for three reasons. The first of these is the prevalence of Fermi resonances, which affect the upper states of the transitions concerned, more particularly, those derived from the symmetric stretches of CH_2 or CH_3 groups. The second reason is the presence of bond strength asymmetry within a CH_2 or CH_3 group, in certain species, which means that the terms symmetric and antisymmetric may no longer be appropriate to the descriptions of the stretching modes in these groups. The third reason is the contribution of two conformers to each of the spectra of the 1,2-, 1,1,2-, and 1,1,2,2- substituted compounds. In at least one case, that of 1,2-difluoroethane, the assignment of observed bands to the different conformers is in dispute. [2,4,19]

The principal tool enabling a correct analysis of this region of the spectrum has proven to be the use of spectra from partially deuterated materials giving the so-called isolated stretching frequencies, ν^{is}CH, hopefully obtained from bands unaffected by Fermi resonances.[23] Unfortunately, problems associated with the preparation of isotopically labeled material appear to have inhibited such studies among the fluoroethanes except for the two cases of monofluoroethane [1,24] and 1,1,1,-trifluoroethane.[3] In this situation, it is natural to enquire if ab initio or density functional theory (DFT) methods offer an alternative approach; this is the first objective of the present work.

For this approach to be successful there are two prerequisites: (1) The quantum-chemical (QC) force field must be scaled with precision, which can only be achieved if suitable frequencies that are free from Fermi resonance effects can be observed. (2) The QC force field must yield reliable CH stretch/CH stretch interaction force constants f' which, along with G matrix terms dependent only on geometry, determine the spacings between different types of CH stretching motion.

Scaling of the force field is necesssary because of the combined effects of imperfection in the level of theory applied and anharmonicity in the vibrational force field of the actual molecule. In all but one of the previous studies of the fluoroethanes, such scaling has taken the form of factors applied to the output frequencies, which are either fixed to one or two chosen values (excluding torsions) [13,16,19,21] or determined by a linear relationship to absolute frequency.[20,22] A preferable procedure is to scale the force field based on internal coordinates to which the QC Cartesian force field may be readily transformed.[25] Such a study has recently been carried out by Baker and Pulay, using the hybrid B3PW91 density functional and a limited number of scale factors associated with "primitive" stretching and bending internal coordinates, these factors being assumed to be common to fluorocarbons in general.[17] However, studies that have been made in this way on molecules for which experimental ν^{is}CH or ν^{is}SiH data are available show that differing scale factors are in fact required for stretching motion for different types of CH or SiH bond. [26−31] A single scale factor applied to either the frequencies or the force constants of such bonds, as in the work of Baker and Pulay, can lead to seriously wrong descriptions of the normal coordinates. In the absence of ν^{is}CH data, this situation may be remedied if bands can be identified that are free of Fermi resonance. For preference, these bands should also be associated with the stretching of only a single type of CH bond.

The second prequisite mentioned above for the successful analysis of the νCH region is a reliable QC calculation of the interaction force constants f'. Studies made so far indicate that HF and DFT calculations perform well in this respect, the main

10.1021/jp001605k CCC: $19.00
Published on Web 09/08/2000

TABLE 1: Observed, Predicted, and Calculated Isolated CH Stretching Frequencies and Calculated CH Bond Lengths

species[a]	bond[a]	ν^{is}CH/cm^{-1}			r_eCH/Å		
		obs[b]	pred[c]	scaled QC[d]	HF[e]	MP2[e]	B3LYP[e]
0	CH	2951.3			1.086 19	1.093 34	1.093 56
1	CH^{x}	2950.2		2948, 2948	1.083 46	1.093 49	1.094 06
1	CH_{g}	2973.5		2974, 2975	1.084 69	1.092 00	1.092 26
1	CH_{t}	2957.0		2966, 2967	1.086 34	1.093 79	1.094 06
11	CH^{xx}		2975	2978, 2978	1.080 47	1.092 08	1.093 32
11	CH_{gg}		2988[f]	2990, 2991	1.083 70	1.091 24	1.091 39
11	CH_{gt}		2989[f]	2989, 2990	1.083 73	1.091 17	1.091 42
12T	CH^{x}_{g}		2977	2963, 2965	1.082 01	1.091 96	1.092 58
12G	CH^{x}_{g}		2965	2964, 2964	1.082 49	1.092 72	1.093 37
12G	CH^{x}_{t}		2936	2943, 2946	1.084 23	1.094 59	1.095 31
111	CH_{ggt}	3010		3011, 3011	1.082 02	1.089 66	1.089 82
112C$_s$	CH^{xx}_{t}		2947	?	1.081 98	1.093 86	1.095 45
112C$_s$	CH^{x}_{gt}		2964	?	1.082 65	1.092 80	1.093 70
112C$_1$	CH^{xx}_{g}		2990	2990, 2990	1.079 56	1.091 11	1.092 53
112C$_1$	CH^{x}_{gg}		2979	2974, 2975	1.081 69	1.091 79	1.092 48
112C$_1$	CH^{x}_{gt}		2982	2973, 2983	1.081 54	1.091 59	1.092 34
1112	CH^{x}_{ggt}		2994	2985, 2995	1.080 81	1.090 85	1.091 73
1122T	CH^{xx}_{gt}		2994	2995, 2995	1.079 39	1.090 84	1.092 35
1122G	CH^{xx}_{gt}		2984	?	1.079 94	1.091 46	1.093 04
11122	CH^{xx}_{ggt}	3001.7			1.079 10	1.090 47	1.092 21

[a] For nomenclature, see text. [b] From references (1,3,24). [c] From the r_e(MP2) correlation[39] with ν^{is}CH(obs) for CH, CH^{x}, CH^{xx}, except where otherwise indicated. [d] This work, from the scaled QC calculations: B3LYP/tz (first datum), HF/tz (second datum). [e] 6-311G** calculations, this work and reference (39). [f] From the r_e(HF/tz) correlation with ν^{is}CH(obs) for CH type bonds only.[39]

criterion being the prediction of sensible Fermi resonance shifts on symmetric CH_3 stretching levels.[27−29] However, in at least one case, MP2 calculations appear to be less satisfactory.[32]

The second objective of the present work was to obtain ν^{is}-CH values additional to the four already known from experiment. These can be output following a successful scaling of a QC force field. They are of interest not only because they provide a direct measure of the strengths of individual CH bonds but also because of the information they provide on the lengths of these bonds.

The great difficulty in obtaining accurate and consistent CH distances experimentally means that the existence of precise correlations between experimental ν^{is}CH and bond length values is of great importance.[23,33,34] The earlier of these involved r_0 values,[33] the more recent, r_e ones.[34] Local mode CH frequencies also give rise to a valuable correlation of this kind.[35] Similar correlations have been made between ν^{is}CH (obs) and CH distance calculated ab initio. Those calculated for hydrocarbons at the HF level are remarkably precise,[36−38] although the variation with basis set in the gradient of such correlations is a matter for concern.[38] A similar exploration was included in a recent study by ab initio and DFT methods of bond lengths in fluoro- and chloroethanes and disilanes.[39] By contrast with the hydrocarbon studies cited above, a close correlation between QC CH bond length and observed ν^{is}CH value was only evident where variations arose from the vicinal gauche or trans effects of halogen (fluorine or chlorine) on the remote carbon atom. A different correlation of this kind was usually needed for each set of CH bonds with zero, one or two geminal halogens, respectively. The best fit to the sparse ν^{is}CH data currently available for fluoroethanes was obtained using bond lengths calculated at the MP2/6-311G** level. (This level and basis set produces CH bond length changes in exact agreement with r_e ones determined experimentally.[34]) This fit was then used to predict ν^{is}CH values for all the unobserved cases. The resulting predictions together with the six experimental values of ν^{is}CH, are listed in Table 1. Despite the low precision expected for them, they proved to be an important guide in the analysis of the spectra where two conformers are present.

The fresh "indirect" values of ν^{is}CH obtained in the course of the present study should increase the precision of predictions via the correlations with bond length for those remaining undetermined.

The third objective of this work, related to that just described, was to explore the relation between bond length and valence stretching force constant f for all three types of bond present, CH, CF, and CC. Such constants are readily available from a QC force field. Stretch−stretch interaction constants f' are also of interest in identifying long-range interactions between bonds that are sensitive to conformation.[32,40] Such interactions are often indiscernible in actual spectra. For CH bonds, f' values are an essential component of local mode analyses.[35]

A fourth objective was to throw further light on assignments that are lower in the spectrum, especially in the region 1200−1000 cm^{-1}. Despite the number of recent QC studies, a close inspection of the available experimental data reveals continuing uncertainty over some assignments as well as a need for a more precise prediction of unobserved modes, especially in the conformers of the 1,2-, 1,1,2-, and 1,1,2,2- fluoro-compounds, which are present only in small proportions in the gaseous or liquid phases. For the latter purpose, DFT calculations are to be preferred because their scale factors are closer to unity than those for the HF or MP2 ones employed previously.[17,41] Although those of Pulay and Baker have significantly improved our understanding in this respect,[17] a further improvement may be anticipated if an increased number of scale factors is calculated for the more abundant conformer of a specific compound and these then transferred to the less abundant form, instead of attempting to fit the entire series of fluorocarbons with a single set of six factors.

Theoretical

Ab initio and DFT calculations were carried out using the program Gaussian 94.[42] Optimization and force constant calculations were made throughout the series at two levels, Hartree−Fock and B3LYP,[43−45] both with the basis set 6-311G**. For monofluoroethane additional calculations were carried out with the 6-31G* basis set and at the MP2 level as detailed elsewhere.[39] In all cases the "tight" condition for optimization in the Gaussian input was employed togther with an SCF convergence limit of 10^{-10}. Test runs showed that under these conditions CH and CF bond lengths converged from differing starting geometries to final values agreeing to within 0.000 02 Å, for the CC bond, the corresponding figure was 0.000 05 Å. The relevance to the calculation of CH stretching frequencies is seen when it is appreciated that a change in CH bond length of 0.001 Å, the accuracy normally quoted for a bond length in QC publications, corresponds to a change in ν^{is}CH of about 7 cm^{-1}.[34]

For the calculation of the force field in internal coordinates and subsequent scaling, the QC output of Cartesian force constants and atomic coordinates was input into the program ASYM40,[46] which scales force constants according to the procedure recommended by Pulay et al.[25] Off-diagonal constants are multiplied by the geometric mean of those associated with the corresponding two diagonal constants.

A standard set of internal coordinates was used, which differ from those advocated by Pulay et al.[25] in a few cases, as shown in the Appendix.

For a thorough scaling of the force field, frequency data from a number of isotopomers is normally needed, and this information is lacking for nearly all of the fluoroethanes. However, with DFT-based force fields, where the scale factors are in any case

close to unity, the lack of isotopic data is not a critical handicap, except with respect to CH stretching constants. A general feature of the B3LYP fluoroethane calculations, where isotopic data were unavailable, was an inability to define a scale factor for CC stretching. This factor was usually found to be highly correlated with the factors for CF stretching. In these cases, the νCC factor was therefore constrained to unity.

Nomenclature

It is convenient to employ the same systems for designating molecules and bonds as has been used previously.[39]

Each molecule is identified by the number of halogen atoms present, and (if necessary) point group, as follows: C_2H_6 **0**(D_{3d}); C_2H_5X **1**(C_s); 1,1-$C_2H_4X_2$ **11**(C_s); 1,2-$C_2H_4X_2$ **12T** (trans, C_{2h}) or **12G** (gauche, C_2); 1,1,1-$C_2H_3X_3$ **111**(C_{3v}); 1,1,2-$C_2H_3X_3$ **112C$_s$** or **112C$_1$**; 1,1,1,2-$C_2H_2X_4$ **1112**; 1,1,2,2,-$C_2H_2X_4$ **1122T** (C_{2h}) or **1122G** (C_2); 1,1,1,2,2-C_2HX_5 **11122**; and C_2X_6 **111222**.

For brevity in the Tables below, the 6-311G** basis set is designated by tz (triple-ζ).

Each bond or atom in each molecule carries a superscript *x* or *xx* if it is α (gem) to one or two F atoms respectively, and a subscript showing the number of trans (*t*) or gauche (*g*) fluorines. This nomenclature is illustrated by the Newman diagrams in Figure 1, which represent the 10 members of the series where several types of CH or CF bond are present in the same molecule. For a generic symbol for all bonds having the same number of α fluorines, the subscript is omitted.

Results and Discussion

I. Individual Compounds: Assignments and ν^{is}CH Values. The reliability of the proposed method for determining ν^{is}CH values may be tested by first treating the two cases where experimental values of the latter are available, namely **111** and **1** (the solitary CH stretch in **11122** needs no discussion here).

111. Complete sets of frequencies for the d_0 and d_3 isotopomers in the gas phase are found in the work of Bürger et al., which also include the value of ν^{is}CH observed in the d_2 species.[3] Refining a single CH stretching scale factor to the value of 3035 cm^{-1} observed for the antisymmetric stretching mode ν_7 yields a predicted value for ν^{is}CH of 3011 cm^{-1}, from both B3LYP/tz and HF/tz treatments, in excellent agreement with the observed value of 3010 cm^{-1}. [3] At the same time, the symmetric stretch ν_1 is predicted at 2957 cm^{-1} at both levels of theory, which indicates an acceptable Fermi resonance shift of 18 cm^{-1} on the observed value of 2975 cm^{-1}.

Table 2 shows the frequency fit for the two isotopomers of **111** yielded by the refinement of six scale factors, the latter listed in Table 10 below. Three small corrections for obvious Fermi resonances have been made to the observed data.

1. The comprehensive data obtained by Lavalley and coworkers for the d_0, d_2, d_3, and d_5 species[1] provide satisfactory assignments in all but a single case, that of ν_7 in the d_0 isotopomer, which is calculated 24 cm^{-1} lower than the value of 1397 cm^{-1} previously given. (The new value of 1373 cm^{-1} explains a shoulder seen at 1368 cm^{-1} in solution.) Experimental ν^{is}CH data and empirical valence force constants were published in references (24) and (47), respectively. Details of the force field and accompanying structures will hopefully be reported elsewhere,[48] but the corresponding B3LYP/tz scale factors are given below in Table 10.

Here, we concentrate on the ν^{is}CH factors which are collected in part A of Table 3. Bearing in mind the precision of the experimental ν^{is}CH values, the factors based on the latter for the stretching of the CH$_g$ and CH$_t$ bonds in the methyl group

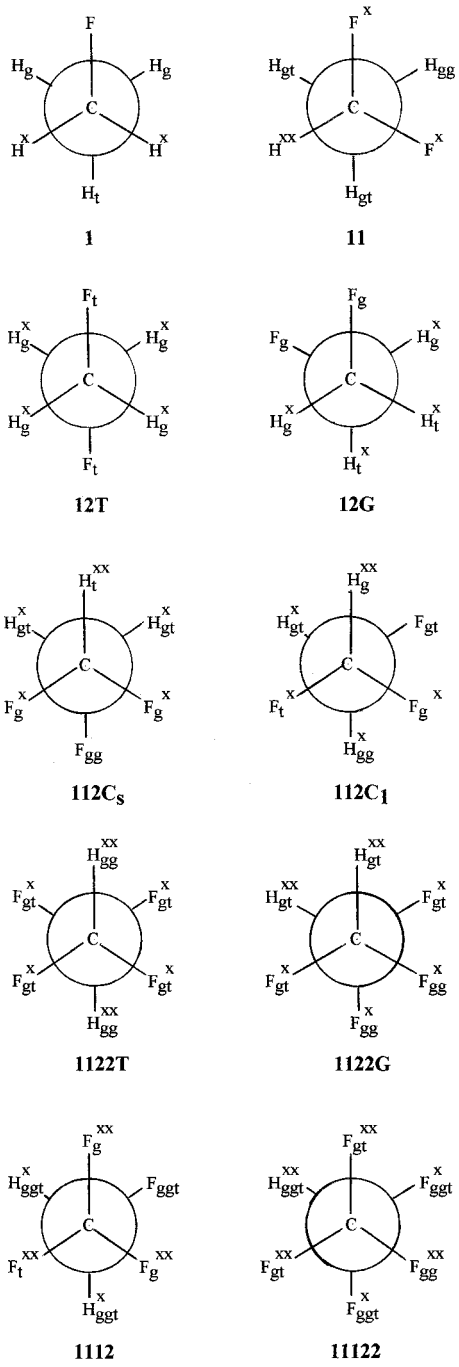

Figure 1. Newman diagrams for ten $C_2H_{6-N}F_N$ type molecules, showing different types of CH and CF bond. Superscripts *x* and subscripts *g* and *t* indicate the numbers of fluorine atoms α, gauche or trans to each bond.

are significantly different from each other at both levels of calculation. More striking is the change in the scale factor for the CH^x bond in the methylene group relative to those in the methyl one, on passing from the HF calculation to the B3LYP one. This reflects the marked lengthening of the CH bond due to α fluorine which is a feature of calculations that include electron correlation, by either MP2 or DFT approaches.[17,39]

The problem involved in attempting to scale the three different kinds of CH bond stretching, without use of the observed ν^{is}-CH data, stems from the fact that there are only two CH stretching bands in the symmetric isotopomers that are both likely to be free of Fermi resonance and also involve one kind of CH bond only. These are the A" bands ν_{12} in the d_2 and d_3 isotopomers, which respectively involve antisymmetric stretch-

TABLE 2: Calculated and Observed Frequencies (cm^{-1}) in 111

mode		**111**-d_0				**111**-d_3		
		ν_{unsc}[a]	A[b]	ν_{obs}[c]	ϵ_ν[d]	ν_{unsc}[a]	ν_{obs}[c]	ϵ_ν[d]
A_1	1	3066	7	2975	(2956.6)	2203	2171	(2125.2)
	2	1433	86	1416[e]	0.7	1323	1324	−4.4
	3	1282	181	1282	−4.5	1083	1071	0.2
	4	826	6	831	1.5	794	799	2.2
	5	595	22	606	3.7	563	572	3.3
A_2	6	230	0	220	0.0	165	162	3.7
E	7	3148	12	3035[f]	0.0	2334	2282	(2250.8)
	8	1482	1	1457	−3.0	1195	1202	−2.4
	9	1232	476	1233	−4.2	1062	1047[e]	2.0
	10	967	142	970[e]	2.2	811	813	1.2
	11	535	1	544	0.6	518	524	−2.3
	12	362	1	367	−1.0	330	335	−0.1
ν^{is}CH		3123		3010	(3011.0)			

[a] Unscaled frequency from the B3LYP/tz calculation. [b] Calculated infrared intensity in km mol^{-1}. [c] Frequencies from reference (3). [d] Error vector $\nu_{obs} - \nu_{calc}$, six scale factors refined. In parentheses, the calculated frequency. [e] Fermi resonance correction applied.[6] [f] Frequency used to scale νCH.

TABLE 3: Calculated and Observed CH Stretching Frequencies (cm^{-1}) in 1

A. ν^{is}_{CH} and scale factors

	unscaled			scaled[b]	
bond	B3LYP/tz	HF/tz	ν^{is}CH observed[a]	B3LYP/tz	HF/tz
CH^x	3055	3230	2950.2	2948	2948
CH_g	3086	3223	2973.5	2974	2975
CH_t	3073	3209	2957.0	2966	2967
	scale factor[c]			scale factor[b]	
CH^x	0.9323	0.8341		0.9306	0.8331
CH_g	0.9282	0.8509		0.9285	0.8519
CH_t	0.9261	0.8489		0.9318	0.8546

B. CH stretching frequencies in the d_0, d_2 and d_3 species and scaled force field fit

		ϵ_ν[e]	
species/sym	νCH(obs)[d]	B3LYP/tz	HF/tz
d_0 A′	2990(5)	0.1	0.2
A′	?	(2926.1)	(2931.3)
A′	?	(2923.6)	(2923.5)
A"	2999.1(20)	−0.9	−0.8
A"	2964.4(20)	1.9	1.8
d_2 A′	2989(5)	−0.1	−0.2
A′	?	(2925.3)	(2928.6)
A"	2996(3)	1.2	1.0
d_3 A′	?	(2925.1)	(2927.0)
A"	2966.5(20)	−1.5	−1.4

[a] From reference (24). [b] Values from scaling to the data in Part B. [c] Scale factors fitting observed values of ν^{is}CH. [d] Data from reference (1). In parentheses, the uncertainty assumed. [e] $\nu_{obs} - \nu_{calc}$: in parentheses, the calculated frequency.

ing of the CH_g and CH^x pairs of bonds. A scale factor refinement based on these bands, on the A" CH stretching bands of the parent d_0 species and on the highest A′ mode in d_0 and d_2, as shown in part B of Table 3, yields the predicted ν^{is} values shown in columns five and six of part A. Here, it is seen that the CH_t value is 9 cm^{-1} too high. The magnitude of the latter error is not unexpected because the only information regarding the value of $\nu^{is}CH_t$ is derived from the two A′ frequencies where Fermi resonance is more likely to be present and where the proportion of CH_t stretching is minor. (A small resonance also appears to affect the A" band in the d_2 species).

Taken together, the results for ν^{is}CH from **111** and **1** indicate that the present procedure for determining ν^{is}CH is likely to be satisfactory in most instances.

11. The infrared frequencies available here (Table 4) are unusually precise, all but four having been obtained from jet-cooled FTIR spectra.[8] Only two fundamentals are not observed in IR spectra, ν_{12} and ν_{13} in the A" symmetry species. The former has been identified with the weak Raman band seen at 3001 cm^{-1} in the gas phase, whereas the latter is a methyl antisymmetric deformation that is predicted to lie within 4 cm^{-1} of the A′ mode at 1457.0 cm^{-1}. A feature of the B3LYP scaled force field is its inability to reproduce the relative magnitudes of ν_8 (1145.1 cm^{-1}) and ν_{15} (1135.0 cm^{-1}), despite the large number (8) of scale factors employed. This is a feature also of unscaled MP2 calculations.[12,14,18] For this reason, a fit with the assignments of these two bands reversed is included in Table 4. Such a reassignment would necessitate a reinterpretation of the contours of the two IR bands concerned.[8] Whether a second-order Coriolis effect could be responsible, merits attention.

TABLE 4: Calculated and Observed Frequencies (cm^{-1}) in 11

mode	ν_{unsc}[a]	A[b]	ν_{obs}[c]	ϵ_ν[d,e]	ϵ_ν[d,f]	ϵ_ν[d,e,g]
			A′			
1	3130	20	3016.1	0.0	0.0	0.0
2	3071	43	2975.2	0.0	0.0	0.0
3	3050	4	2958.5	(2937.8)	(2932.2)	(2937.9)
4	1482	5	1457.0	2.6	2.6	2.0
5	1436	79	1413.2	−1.4	−1.4	−0.3
6	1388	6	1359.8	−4.3	−4.3	−3.5
7	1161	35	1171.1	6.5	6.5	2.3
8	1133	108	1145.1(1135.0)	11.0	11.0	4.0
9	871	9	868.7	− 0.1	− 0.1	−1.1
10	563	7	569.9	−3.3	−3.3	−3.0
11	463	13	470.1	0.3	0.3	−1.1
			A"			
12	3126	13	3001	(3011.0)	0.0	(3011.0)
13	1485	1	?	(1456.7)	(1456.7)	(1457.1)
14	1396	25	1364.1	1.4	1.4	1.1
15	1145	131	1135.0(1145.1)	−9.1	−9.1	−0.4
16	944	81	941.8	0.0	0.0	−0.9
17	381	0	390.5	1.1	1.1	1.1
18	241	0	221	0.0	0.0	0.0
$\nu^{is}CH^{xx}$	3073			(2978.0)	(2977.9)	(2978.0)
$\nu^{is}CH_{gg}$	3104			(2989.9)	(2994.2)	(2989.0)
$\nu^{is}CH_{gt}$	3101			(2989.1)	(2979.2)	(2989.1)

[a] Unscaled frequencies from the B3LYP/tz calculation. [b] Computed infrared intensity in km mol^{-1}. [c] Data from reference (8). In parentheses, the reversed assignment fitted in column seven. [d] $\nu_{obs} - \nu_{calc}$. In parentheses, the calculated frequency. [e] Eight scale factors refined, (3001 cm^{-1} omitted). [f] Nine scale factors refined, (3001 cm^{-1} included). [g] $\nu_8 \rightarrow$ 1135 cm^{-1}; $\nu_{15} \rightarrow$ 1145.1 cm^{-1}.

Turning to the CH stretching region, the problem here is fitting the split components of $\nu_{as}CH_3$ at 3016.1 (A′) and 3001 (A") cm^{-1}. The band at 2975.2 cm^{-1} is clearly primarily due to νCH^{xx}, whereas that at 2958.5 cm^{-1} is similarly associated with ν_sCH_3, displaced upward by about 20 cm^{-1} by the usual Fermi resonance with a $2 \times \delta_{as}CH_3$ level.

From the recent geometry optimization studies,[39] both B3LYP and HF treatments are expected to entail differing scale factors for the stretching of the CH^{xx} and methyl group bonds. However, the virtual identity of the CH_{gg} and CH_{gt} bond lengths suggests that their isolated frequencies will be identical and their scale factors the same. However, it proves impossible to fit the three highest frequencies on this assumption.

The data in column five of Table 4 show that fitting the more precise data, 3016.0(ν_1) and 2975.2(ν_2) cm^{-1} , with just two νCH scale factors, yields ν^{is}CH values which are very close to those predicted in Table 1. The Fermi resonance shift on ν_3 is then an acceptable 21 cm^{-1}. However ν_{12} is predicted 10 cm^{-1} higher than the broad weak Raman band at 3001 cm^{-1}.

Column six of Table 4 shows the effect of fitting the latter band as ν_{12}, as well as ν_1 and ν_2, three scale factors then being necessary. The Fermi resonance shift on ν_3 increases to about 26 cm^{-1}, which is not impossible, but the 15 cm^{-1} difference in ν^{is} for the two kinds of bond in the methyl group is worrying,

TABLE 5: Calculated and Observed Frequencies (cm^{-1}) in 12G and 12T

	12G					12T				
mode		ν_{unsc}[a]	A[b]	ν_{obs}[c]	ϵ_ν[d]		ν_{unsc}[a]	A[b]	ν_{pred}[e]	ν_{pred}[f]	ν_{obs}[c]
1	A	3083	19	2974	(2972.6)	A_g	3048		2938	2931	
2		3039	39	2958	(2929.9)		1516		1488	1493	
3		1490	0	n.o.	(1461.7)		1457		1423	1436	
4		1442	14	1410	−0.8		1083		1085	1077	
5		1304	2	1286	−0.3		1053		1055	1059	1052
6		1128	1	1116	−0.7		455		460	460	457
7		1102	85	1100	0.0	A_u	3118	62	3001	2998	3001[g]
8		870	29	864	−0.9		1233	4	1216	1208	1218[h]
9		320	0	326	1.3		827	0	813	799	
10		150	4	147	0.1		123	14	120	133	117
11	B	3097	46	2986[g]	0.0	B_g	3091		2980	2973	
12		3028	13		(2918.8)		1299		1281	1276	
13		1487	9	1459	0.0		1178		1158	1158	
14		1410	9	1376	0.8	B_u	3054	64	2944	2936	
15		1261	5	1244	0.4		1525	2	1496	1502	1490[h]
16		1080	46	1078	0.7		1369	10	1336	1342	
17		903	48	896	−0.3		1061	204	1062	1076	1060
18		493	17	499	1.9		279	20	283	279	285
$\nu^{is}CH^x{}_g$		3074			(2963.6)		3078		(2963.4)		
$\nu^{is}\ CH^x{}_t$		3052			(2942.5)						

[a] From the B3LYP/tz calculation. [b] Computed infrared intensity in km mol^{-1}. [c] Frequencies observed in references (2,4,19). [d] $\nu_{obs} - \nu_{calc}$: in parentheses, the calculated frequency. Eight scale factors refined. [e] Predicted using the **12G** scale factors, except for νCH. [f] Scaled B3PWP91 prediction.[17] [g] Frequency used for scaling νCH. [h] Argon matrix frequency.

TABLE 6: Calculated and Observed Frequencies (cm^{-1}) in 112

	$112C_1$					$112C_s$				
mode	ν_{unsc}[a]	A[b]	ν_{obs}[c]	ϵ_ν[d]		ν_{unsc}[a]	A[b]	ν_{pred}[e]	ν_{pred}[f]	ν_{obs}[c]
1	3119	30	3005[g]	0.0	A′	3059	63	2959	2942	2979?[g]
2	3088	26	2986[g]	0.0		3042	5	2930	2926	2968?
3	3057	17	2978	(2942.8)		1489	7	1454	1473	1460
4	1494	3	1465	2.9		1432	15	1409	1415	1419
5	1454	15	1433	−5.8		1411	29	1384	1399	1394
6	1409	20	1373	0.2		1172	129	1176	1161	1177?
7	1344	18	1319	1.2		1090	24	1096	1096	1100?
8	1264	10	1250	−2.1		870	37	867	859	869
9	1148	90	1155	0.5		755	54	764	761	756
10	1133	9	1125	−2.0		512	12	518	516	517
11	1094	60	1100	0.4		233	2	235	229	?
12	1075	23	1076	0.4	A"	3099	22	2983	2983	2997?[g]
13	906	42	905	−0.1		1396	26	1360	1389	1361[h]
14	573	4	577	−1.3		1282	14	1255	1256	1261[h]
15	473	20	476	2.2		1129	102	1127	1138	1148?
16	423	5	426	0.3		947	83	940	950	936[i]
17	243	9	(247)	(242.0)		367	0	370	373	381[i]
18	116	9	117	0.0		116	2	112	106	?
$\nu^{is}\ CH^{xx}{}_g$	3090			(2990.4)	$\nu^{is}\ CH^{xx}{}_t$	3055		2957		(2977.6)[j]
$\nu^{is}\ CH^x{}_{gg}$	3089			(2973.7)	$\nu^{is}\ CH^x{}_{gt}$	3073		2959		(2972.5)[j]
$\nu^{is}\ CH^x{}_{gt}$	3088			(2973.0)						

[a] From the unscaled B3LYP/tz calculation. [b] Computed infrared intensity in km mol^{-1}. [c] Frequencies observed in reference (5), as assigned by Baker and Pulay[17], except for νCH in **$112C_s$**. [d] $\nu_{obs} - \nu_{calc}$: in parentheses, the calculated frequency, using nine scale factors. [e] Predicted using scale factors transferred from **$112C_1$**. [f] Scaled B3PW91 prediction.[17] [e] Frequency used for scaling νCH. [h] Solid-state value. [i] Liquid-state value. [j] From a scaled force field fitting the 2997 and 2979 cm^{-1} frequencies.

because it conflicts with the identity of their bond lengths. In addition, the scale factors for the two CH bonds become significantly different (0.9307 for CH_{gg} and 0.9218 for CH_{gt}) and out of line with those for CH type bonds in the other fluoroethanes, as collected in Table 10 below. For several reasons, therefore, the analysis in column five, which ignores the 3001 cm^{-1} band, is to be preferred. However, it is clear that the previous assignment of the 2975.2 cm^{-1} band to νCH^{xx} is satisfactory and that the ν^{is}CH value of 2978 cm^{-1} for this bond is securely based.

12. The dominant species here is **12G**.[19] As a result, only a limited number of bands can be ascribed to **12T** and the remainder of the latter's fundamentals must be predicted by transferring scale factors from **12G**. Reassignments are needed in several regions of the spectrum, 2900−3010 cm^{-1} and 1050−1200 cm^{-1}.[2,4,19]

Table 5 lists the unscaled B3LYP frequencies and infrared intensities and observed frequencies for both conformers, the fit to the observed data for **12G** from the scaled force field, and frequencies predicted from the latter for **12T**.

In the higher region of the spectrum, no one doubts the assignment of the strong infrared band at 2986 cm^{-1} to ν_{11}(B) of **12G**. Scaling the νCH force constants of both conformers to reproduce this 2986 cm^{-1} band places all the other **12G** frequencies well below 2986 cm^{-1} and only the A_u mode ν_7 of **12T** above, at 3010 cm^{-1}. This, together with convincing evidence from the argon matrix spectrum,[2] identifies the infrared band in the gas phase at 3001 cm^{-1} as due to ν_7 (**12T**). A small change in scale factor is adequate for exact reproduction of this frequency, as seen in Table 10. It is not possible to derive separate scale factors for the two kinds of CH bond in **12G**. The 2986 cm^{-1} mode involves motion in both types of bond to some extent. However, the assumption of a common scale factor leads to prediction of ν_1 at 2973 cm^{-1}, the resulting band being weak in the IR and strong in the Raman spectrum, with a high depolarization ratio (0.74), from the HF calculation. This then

TABLE 7: Calculated and Observed Frequencies (cm^{-1}) in 1112 and 11122

	1112				11122				
mode	ν_{unsc}[a]	A[b]	ν_{obs}[c]	ϵ_ν[d]	ν_{unsc}[a]	A[b]	ν_{obs}[e]	ϵ_ν[d,f]	ϵ_ν[d,g]
				A′					
1	3067	14	2984.1	(2954.7)	3101	23	3002	0.0	0.0
2	1491	5	1464.3	0.0	1436	1	1392	−16.5	−4.6
3	1446	16	1430.0	0.6	1304	165	1310	13.2	3.5
4	1297	165	1294.0	−4.4	1186	209	1199	7.2	4.4
5	1168	291	1185.9	8.3	1134	154	1142	−7.3	−5.8
6	1100	92	1104.6	−3.6	861	52	868	−1.9	−3.4
7	837	11	844.0	0.4	717	35	727	−3.7	−3.2
8	657	33	665.6	−3.9	573	14	578	−4.9	−5.9
9	542	8	549.4	3.5	516	8	523	−4.1	−4.3
10	406	1	409.3	−4.1	358	0	364	0.1	0.3
11	216	3	225	1.5	241	4	250	3.5	3.7
				A"					
12	3127	13	3012.6	0.0	1383	10	1356	0.0	−0.1
13	1308	114	1301.3	−0.9	1202	394	1225	5.0	7.2
14	1197	105	1203.5	3.1	1132	113	1146	−1.1	1.1
15	973	79	974.3	−1.9	576	1	592	4.3	4.5
16	527	2	533.1	2.4	411	1	420	−0.3	−0.4
17	349	1	351.7	−1.3	209	3	212	−2.0	−2.1
18	103	6	109.0	0.1	66	1	75	0.0	0.0
ν^{is}	3099			(2985.2)			3002		

[a] From the B3LYP/tz calculation. [b] Computed infrared intensity in km mol^{-1}. [c] Data from reference (7). [d] $\nu_{obs} - \nu_{calc}$: in parentheses, the calculated frequency. Nine scale factors refined. [e] Data from reference (21). [f] Six scale factors refined. [g] Six scale factors refined, after constraining $F_{\nu CC/\delta CH} = 0.195$ aJ $Å^{-2}$

provides an excellent fit to the Raman band observed at 2974 cm^{-1}. Such a good fit would be surprising if the two scale factors differed appreciably. ν_{11} from **12T** is also expected near 2980 cm^{-1} but with a calculated Raman intensity less than one-fifth of that due to ν_1 in **12G**.

The remaining bands of **12G** are predicted at 2930 (ν_2) and 2919 cm^{-1} (ν_{12}), respectively. The former is surely associated with the band at 2958 cm^{-1}, prominent both in the IR and the Raman spectrum, and several overtone and combination levels can be invoked to account for a large upward displacement due to Fermi resonance from its expected value. The most conspicuous of the latter is the very strong Raman band at 2901 cm^{-1}. The band due to ν_{12} is predicted to be rather less intense than ν_1 in both the IR and Raman spectra and at 2919 cm^{-1} coincides with the B combination 1462 + 1459 cm^{-1}.

The Fermi resonance possibilities in **12T** are more complex than those in **12G** due to two unusually high bending modes present. These are predicted at 1496 (B_u) and 1488 (A_g) cm^{-1}, the former being seen in the argon matrix at 1490 cm^{-1}.[2] Overtones from both of these can account for the polarized Raman line seen at 2995 cm^{-1} in the Raman spectrum, assuming an upward shift due to resonance with ν_1 (A_g), predicted below at 2931 cm^{-1}. An unassigned weak argon matrix band at 2994 cm^{-1} lies suspiciously close to this 2995 cm^{-1} gas-phase band, suggesting that its earlier assignment to **12G** may be in error.[2] There is no binary **12G** combination or overtone level as high as this. This suspicion is reinforced by the fact that the two fundamentals here, ν_7(**12T**) and ν_{11} (**12G**) both rise from gas phase to matrix, by 9 and 12 cm^{-1} respectively, whereas the 2995 cm^{-1} band apparently remains unchanged.

Turning to the other region, 1050−1100 cm^{-1}, where frequencies are in doubt, it is clear from a comparison of spectra from two laboratories, that the infrared bands in the gas phase are hard to interpret.[4,19] Again, the situation is clarified by the extensive studies of infrared spectra in matrixes by Günthard and co-workers.[2,49,50] The prominent bands in argon at 1096, 1070, and 1048 cm^{-1} plainly arise from **12G**, **12G**, and **12T**, respectively, and relate satisfactorily to the gas-phase Raman bands at 1100 and 1078 cm^{-1} and the infrared Q branch at 1060 cm^{-1}.[19] These values lie very close to the frequencies of the strong infrared bands predicted from the unscaled B3LYP force field at 1102 cm^{-1} (**12G**, ν_7), 1080 cm^{-1} (**12G**, ν_{16}), and 1061 cm^{-1}(**12T**, ν_{17}).

With these assignments, the excellent fit to the **12G** data in Table 5 was obtained with the eight scale factors listed in Table 10. As usual, the νCC factor was undefined and had to be constrained to unity. Transferring these factors to the corresponding force constants in the **12T** force field, with the sole exception of an adjustment to the νCH factor, yielded the predicted frequencies of column eight in Table 5. The fit to the eight observed data for **12T** is excellent, suggesting that none of the predicted values is likely to be in error by more than 5 cm^{-1}. The overall precision appears to be a little better than that of the earlier predictions of Baker and Pulay,[17] shown in column nine of Table 5.

A notable result is the prediction of high δCH_2 frequencies in the neighborhood of 1490 cm^{-1} in **12T**, as utilized above.

The whole scaling procedure was then repeated with the HF/tz force field (not shown). A comparable fit to the **12G** frequencies required 10 independent scale factors, including one for νCC and separate ones for the CH_2 wagging coordinates in the A and B symmetry species. One difference from the DFT-based force field was the prediction of ν_{15}(**T**) at 1463 cm^{-1}, substantially below the matrix value of 1490 cm^{-1} assigned above.

We note finally in these conformers that the scaled $\nu^{is}CH_g$ values in **12T** and **12G** are identical at 2963.5(B3LYP) and 2964.5(HF), in contrast to the 12 cm^{-1} spacing previously predicted in Table 1. This means that a significant increase in scale factor for the CH_g bond has occurred from **12T** to **12G**, as seen in Table 10.

The $\nu^{is}CH_t$ value in **12G** is less well defined by the scaling procedure employed, but the lower values of 2942.5(B3LYP) or 2945.7 cm^{-1}(HF) yield a gauche−trans difference of 21 or 19 cm^{-1} which represents a normal conformational effect of β halogen, as seen in **1**, though not apparently in **11**.[23,24]

112. Here, the C_1 conformer is the more abundant species (92% [51]), although the crystal phase contains only the C_s form.[5] For several of the bands of the latter, only solid or liquid-phase frequencies are available. The spectra from **112C$_1$**, therefore, constitute a more complete and precise set.[5] As before, assignment problems arise both in the CH stretching region and also between 1200 and 1050 cm^{-1}.

The predictions of ν^{is}CH values from ab initio CH bond lengths in Table 1 and the computed B3LYP/tz frequencies in Table 6 indicate that the CH stretches in **112C$_1$** should lie well above those in **112C$_s$**. Moreover, the highest band in the **112C$_s$** spectrum should be that due to ν_{12}(A", $\nu_{as}CH_2$). HF, MP2 and B3PW91 calculations lead to the same conclusions.[13,14,17,18] Examining the spectra reported by Kalasinsky et al.,[5] the assignments of the prominent IR bands at 3005 and 2986 cm^{-1} and the strong Raman band at 2974 cm^{-1} to the **112C$_1$** modes ν_1, ν_2, and ν_3 respectively, seem inescapable, bearing in mind the strong upward resonance shift expected on the band due to $\nu_3(\nu_sCH_2)$. This implies that all of the bands of **112C$_s$** should lie below 3005 cm^{-1}. The solid-phase bands near 3037 cm^{-1}, which have to be assigned to **112C$_s$**, must have therefore experienced a large upward phase shift similar to that of 49 cm^{-1} observed in **1122T**.[5] Such a shift is compatible with assignment of the weak Q branch at 2997 cm^{-1} to ν_{12} in **112C$_s$**, previously ascribed to ν_1.[5] However, this Q branch could also be a hot band associated with the intense 3005 cm^{-1} **112C$_1$**

TABLE 8. Calculated and Observed Frequencies (cm^{-1}) in 1122

		1122T					1122G					
mode		ν_{unsc}[a]	A[b]	ν_{obs}[c]	ϵ_ν[d]		ν_{unsc}[a]	A[b]	ν_{pred}[e]	ν_{pred}[f]	ν_{obs}[c]	ϵ_ν[d,g]
1	A_g	3092		2995	1.4	A	3091	42	2992	2974	?	(2992.0)
2		1459		1442	−10.0		1435	2	1432	1427	?	(1432.7)
3		1146		1149	4.9		1392	16	1364	1382	1362	−1.7
4		1107		1106	−8.7		1201	151	1202	1192	1205	−5.9
5		620		625	0.2		1100	25	1104	1118	1119	4.5
6		358		362	0.8		904	47	904	898	906	−0.9
7	A_u	1363	35	1331	−0.5		595	5	601	591	598	−4.7
8		1131	411	1136	2.8		403	2	407	411	408	0.5
9		205	3	210	0.0		246	2	248	245	250	1.6
10		80	2	82	0.0		72	1	74	67	?	(74.1)
11	B_g	1390		1361	0.8	B	3083	21	2984	2965	?	(2984.1)
12		1099		(1081)	(1101.9)		1419	31	1400	1408	1394	−6.0
13		480		480	−4.9		1340	24	1320	1327	1309	−11.4
14	B_u	3103	50	2995	−1.4		1125	32	1130	1138	1146	6.0
15		1317	28	1320	6.0		1121	340	1123	1121	1136	−0.4
16		1123	237	1127.4	0.2		775	77	781	784	780	−3.3
17		537	9	542	−1.4		517	15	522	521	523	0.3
18		410	51	413	0.9		232	6	235	231	?	(235.1)
ν^{is} CH^{xx}_{gg}		3098			(2995.0)							
ν^{is} CH^{xx}_{gt}							3087					(2988.0)

[a] From the B3LYP/tz calculation. [b] Computed infrared intensity in km mol^{-1}. [c] Frequencies observed in references (5,11). [d] $\nu_{obs} - \nu_{calc}$: in parentheses, the calculated frequency. Six scale factors refined. [e] Predicted using the **12T** scale factors. [f] Scaled B3PW91 prediction.[17] [g] Error vector after refinement of the νCF scale factor only.

TABLE 9: Observed Frequencies (cm^{-1}) and Frequency Fit for Scaled B3LYP/tz Calculations, for 0 and 111222

		0			111222		
mode		ν_{obs} [a]	$\epsilon_\nu(4)$[b]	$\epsilon_\nu(5)$[b]	ν_{obs}	$\epsilon_\nu(3)$[b]	$\epsilon_\nu(4)$[b]
A_{1g}	1	2920	7.6	7.6	1417[c]	2.2	5.3
	2	1388.4	−2.7	−3.2	807[c]	−3.2	1.2
	3	994.8	−1.9	−1.9	348[c]	2.7	2.7
A_u	4	289	0.0	0.0	67.5[d]	0.0	0.0
A_{2u}	5	2915	2.1	2.1	1117.1[e]	−9.2	−3.4
	6	1379.2	4.7	4.2	714[f]	−2.1	−0.4
E_u	7	2977.7	−3.4	−3.4	1253.0[e]	2.0	−5.1
	8	1471.6	0.3	−0.7	522.5[f]	−0.5	−1.0
	9	821.6	6.5	0.0	220[g]	3.9	3.8
E_g	10	2955.0	−1.7	−1.7	1250[c,h]	12.8	7.4
	11	1468.1	−1.6	−0.4	619[c,h]	1.5	0.2
	12	1190	−9.9	0.0	372[c,h]	−7.9	−8.1
	ν^{is}CH	2951.3	0.0	0.0			

[a] Reference (54). [b] ν_{obs} - ν_{calc}: in parentheses, the number of scale factors refined. [c] Reference (55). [d] Reference (57). [e] Reference (9). [f] Reference (58). [g] Reference (59). [h] Liquid values: 1237, 620, 380 cm^{-1}.[56]

fundamental, in which case the pair of Q branches 2980 and 2978 cm^{-1} would be candidates for the highest **112C$_s$** mode.

The above assigned values of ν_1 and ν_2 in **112C$_1$** were used to scale the CH stretches in this conformer, with the unavoidable assumption that the same factor was used for both CH^x bonds, and these factors then transferred along with the remaining factors to predict all the frequencies in **112C$_s$**, as seen in column eight of Table 6. The three CH stretches concerned are then 2983 cm^{-1} (ν_{12}), 2959 cm^{-1} (ν_1) and 2930 cm^{-1} (ν_2). Therefore, these predictions favor the choice of 2980 cm^{-1} for ν_{12} in **112C$_s$**, which suggests that the 2997 cm^{-1} branch is indeed a hot band. However, the resulting shift of 57 cm^{-1} to the crystal phase value of 3037 cm^{-1} is disturbingly high. The lowest CH stretch (ν_2) in **112C$_s$** would appear to occur at 2968 cm^{-1} from the Raman spectrum, which suggests that the fall in ν^{is}CH from **112C$_1$** to **112C$_s$** is not as great as has been calculated. Estimates of the extent of Fermi resonance on the lowest CH stretch (ν_s-CH_2) in each conformer must remain uncertain until firmer evidence is available, but the concentration of Raman intensity above 2970 cm^{-1} indicates that it must be considerable. At least four levels in each conformer are likely to be involved.

The values of ν^{is}CH shown in Table 6 are based on assigning the pairs of bands 3005, 2986 and 2997, 2979 cm-1 to the two highest **112C$_1$** and **112C$_s$** modes, respectively. They show that although the **112C$_1$** values are nicely compatible with the predictions from bond lengths in Table 1, those for **112C$_s$** are not so. A similar result comes from an accompanying HF/tz study. Until firmer evidence is available for assigning the **112C$_s$** bands, values of ν^{is}CH for this conformer must remain uncertain.

In the 1200−1050 cm^{-1} region, two publications[5,17] have drawn attention to the strong evidence for supposing that the strong IR band at 1100 cm^{-1} in the gas and 1098 cm^{-1} in the crystal involves a fundamental from both conformers, which must include ν_{11} in **112C$_1$** , with ν_{12} at 1076 cm^{-1} and the solid band at 1038 cm^{-1} rejected as a **112C$_1$** fundamental. Table 6 shows that this revised assignment is well reproduced by a nine scale factor force field in which slightly different factors are required for the CF^x and CF bonds, as seen in Table 10. The transfer of these scale factors (the average for the νCF^x values) to **112C$_s$** yields the predicted values in column eight of Table 6, which are compared in column nine of Table 10 to the predictions made with the same **112C$_1$** assignments by Baker and Pulay.[17] The previously unassigned very weak IR band at 1177 cm^{-1} is nicely accounted for by ν_6, but the reproduction of the band seen at 1148 cm^{-1} by ν_{15} is disturbingly poor.

A major difficulty with these revised assignments, not discussed by Baker and Pulay, is that in **112C$_s$**, ν_6 is predicted to give rise to the strongest IR band in the spectrum, yet the IR band observed at 1180 cm^{-1} in the crystal is very weak. By contrast, there is a very strong IR band in the crystal at 1042 cm^{-1}, which surely represents a **112C$_s$** fundamental.

There appear to be only two possible solutions to the problem. Either there is a series of large downward frequency shifts from gas to crystal, such that the **112C$_s$** gas-phase bands 1177, 1148, and 1100 cm^{-1} move to 1140, 1098, and 1042 cm^{-1} in the crystal, or else the νCF scale factors fall significantly from **112C$_1$** to **112C$_s$**.

A similar dilemma is identified above in respect of the CH stretches. Either the νCH scale factors increase significantly

TABLE 10: B3LYP/tz Scale Factors in Fluoroethanes

A. CH stretches

species	CH	CH	CH^x	CH^x	CH^{xx}
0	0.9269				
1	0.9282(*g*)	0.9261(*t*)	0.9323		
11	0.9280(*gg*)[a]	0.9280(*gt*)[a]			0.9389
12T			0.9268(*g*)		
12G			0.9295(*g*)[a]	0.9295(*t*)[a]	
111	0.9292(*ggt*)				
112C$_1$			0.9268(*gg*)[a]	0.9268(*gt*)[a]	0.9364(*g*)
1112			0.9280(*ggt*)		
1122T					0.9370(*gg*)
11122					0.9372(*ggt*)

B. Other coordinates

coord	**0**	**1**	**11**[b]	**11**[c]	**12G**	**111**	**112C$_1$**	**1112**	**1122T**	**11122**	**111222**
$\delta_{as}CH_3$	0.9520[a]	0.9603	0.9610[a]	0.9585[a]		0.9669[a]					
δ_sCH_3	0.9520[a]	0.9571	0.9610[a]	0.9585[a]		0.9669[a]					
$\rho'CH_3$	0.9874[d]	0.9529	0.9754[a]	1.0022[a]		0.9911					
ρ"CH_3	0.9530[e]	0.9741	0.9754[a]	1.0022[a]							
δ_sCH_2		0.9601			0.9636		0.9555[a]	0.9656			
wCH_2		0.9553			0.9509		0.9555[a]	0.9696			
τCH_2		0.9711			0.9730		0.9555[a]	0.9805			
ρCH_2		0.9909			0.9662		0.9555[a]	1.0093			
δ'CH			0.9498[a]	0.9511[a]			0.9443[a]		0.9806	0.8997	
δ"CH			0.9498[a]	0.9511[a]			0.9443[a]		0.9547	0.9569	
νCC	1.0[f]	1.0083	1.0[f]	1.0[f]	1.0[f]	1.0[f]	1.0[f]	1.0[f]	1.0[f]	1.0[f]	1.0[f]
νCF		1.0077			0.9991		1.0125	1.0093[a]			
νCF							1.0335				
νCF^x			1.0135	0.9973			0.9995	1.0093[a]	1.0036	1.0265[a]	
ν_sCF^{xx}						1.0141[a]		1.0093[a]		1.0265[a]	1.0181
$\nu_{as}CF^{xx}$						1.0141[a]		1.0093[a]		1.0265[a]	1.0470
δCF		1.0443	1.0544	1.0518	1.0304		1.0132	1.1420	1.0255	1.0452[a]	
δCF_3[g]						1.0368		1.0168		1.0452[a]	1.0285
torsion	0.8852	0.8635	0.8404	0.8404	0.9467	0.9170	1.0006	1.1182	1.0585	1.2845	1.4630

[a] Sets of factors constrained equal. [b] Assignment as in column four, Table 4, and reference (7). [c] Assignment of 1135 and 1145 cm^{-1} bands reversed. [d] E_u species in ethane. [e] E_g species in ethane. [f] Constrained. [g] Includes δ_{as}, δ_s, and ρCF_3 coordinates.

from **112C$_1$** to **112C$_s$**, to accommodate the 2997 cm^{-1} band as ν_{12} in **112C$_s$**, or a large upward shift of 57 cm^{-1} has occurred in ν_{12} from a gas-phase value of about 2980 cm^{-1} to the crystal frequency of 3037 cm^{-1}.

Clearly, there is a pressing need for further investigation, which should include spectra from jet-cooled IR spectra to precisely define the frequencies of **112C$_1$** and also from matrix-isolated samples, which hopefully will repeat the success previously obtained with the conformers of **12**.[2]

1112. Here again, very precise data are available from jet-cooled FTIR spectra.[6] With only one type of CH bond present, the scaling of CH stretching is simple. Basing the latter on the antisymmetric CH_2 stretching mode ν_{12} at 3012.6 cm^{-1}, ν^{is}-CH^x_{ggt} is predicted at 2985.2 (B3LYP) or 2983.1 cm^{-1}(HF). ν_1, the symmetric stretch of the CH_2 group, is placed at 2954.7-(B3LYP) or 2955.9(HF) cm^{-1}, which yields Fermi resonance corrections of 29.4 or 28.2 cm^{-1} on the observed value of 2984.1 cm^{-1}.

There are no problems with assignment elsewhere in the spectrum. The refinement of nine scale factors yielded the fit seen in Table 7.

1122. The **T** conformer constitutes about 84% of the sample at normal temperatures.[52] The infrared spectrum of Mackenzie shows a dominant C type band at 2995.1 cm^{-1}, with Q branch satellites at 3002.8, 2999.3, 2992.9, and 2991.4 cm^{-1}, all of which are near and weak enough to be hot bands.[53] The main band and the coincident Raman band at 2995 cm^{-1} may confidently be assigned to $\nu_{14}(B_u)$ and $\nu_1(A_g)$ in **1122T**. A near coincidence for these two modes is predicted by the B3LYP calculation, where the interaction force constant $f'_{CH,CH}$ is only -0.003 aJ $Å^{-2}$ (see below). Both unscaled B3LYP and HF calculations predict $\nu^{is}CH^{xx}_{gg}$ in **1122T** to lie about 11 cm^{-1} above $\nu^{is}CH^{xx}_{gt}$ in **1122G**, reflecting a normal gauche − trans effect. In addition, f' becomes positive in **1122G**, so that the more infrared intense band due to $\nu_1(A)$ is predicted to lie about 8 cm^{-1} above $\nu_{11}(B)$, as shown in Table 8. It then becomes difficult to assign the weak Q branch at 3003 cm^{-1} to ν_1 in **1122G** unless there is a significant change in νCH scale factor from **1122T** to **1122G**. If such a change has occurred, then the weaker type B band expected from ν_{11} will underlie the strong **1122T** type C band at 2995 cm^{-1}. More acceptable alternatives for ν_1 in **1122G** are either of the Q branches at 2992.9 or 2991.4 cm^{-1}, with ν_{11} unobserved below.

Elsewhere in the spectrum, the B3LYP frequencies and infrared intensities in Table 8 indicate the need for several further reassignments for **1122G**. $\nu_2(A)$ is predicted to have very little infrared intensity and to lie above $\nu_{12}(B)$, which has been reasonably assigned to the weak infrared band seen at 1394 cm^{-1}. The bands seen at 1362 and 1309 (Raman,1312) cm^{-1} are then respectively $\nu_3(A)$ and $\nu_{13}(B)$, in agreement with Baker and Pulay.[17]

The region 1150−1070 cm^{-1} presents a number of difficulties. Of the three infrared maxima reported, at 1146, 1136, and 1125 cm^{-1}, the first has been assigned to **1122G** on the basis of its disappearance in the solid-phase spectrum. The strongest IR bands in this region should be $\nu_8(A_u)$ and $\nu_{16}(B_u)$ from **1122T**, predicted within 7 cm^{-1} of each other, and the assignments of these made earlier to the 1136 and 1125 cm^{-1} bands seem sensible.[5] However, the former does not have the type B contour expected from an A_u mode. A possible explanation is that a second **1122G** band is making a contribution here. Tentatively, ν_{14} and ν_{15} in **1122G** are assigned to the 1146 cm^{-1} and 1136 cm^{-1} (in part) bands, the distinction in their calculated IR intensities for two modes of the same symmetry predicted as close as 4 cm^{-1} apart probably being illusory.

In checking these assignments with scaled force fields, the well-defined data for **1122T** were first fitted with six scale factors, as seen in Table 8. An extended scaling exploration

failed to fit the 1081 cm^{-1} Raman band previously assigned to $\nu_{12}(B_g)$ [5] and a more likely explanation for this band is the overtone 2×542 cm^{-1} ($2\nu_{17}$) in mild resonance with $\nu_4(A_g)$ above, this resonance increasing from gas to solid phase due to changes in the fundamental frequencies concerned. ν_{12} is then assumed to be unobserved, close to or underlying ν_4. Baker and Pulay[17] also dismiss the 1080 cm^{-1} band as a fundamental but place ν_{12} instead at 1125 cm^{-1}, which would be incompatible with the B3LYP scaled force field. The somewhat imperfect fit in the A_g species is slightly worsened if allowance is made for a small resonance between ν_4 and $2\nu_{17}$ below. Some alleviation can be achieved if the scale factor for CF_2 wagging specific to the A_g species is allowed to vary independently of that for the other CF bending modes. The νCC factor has a negligible effect here. Another source of trouble may be inaccurate off-diagonal symmetry force constants.

Transfer of the six **1122T** scale factors to **1122G** yields the predicted frequencies in column eight of Table 8. The principal anomalies occur with ν_5, ν_{14} and ν_{15}, which are all predicted too low and the fit can be improved by an adjustment of the νCF scale factor, as shown in column eleven. The Baker and Pulay predictions in column nine are better for ν_5 and ν_{14}, but elsewhere, a little poorer than those in the present work.

Fresh IR data in both this region and at 3000 cm^{-1} from jet-cooled and argon matrix studies are again needed to assign a number of these bands.

Lower in the spectrum, both the present study and the earlier ab initio ones[13,14,17,18] make it clear that ν_{18} does not lie at 495 cm^{-1} as previously supposed, but below 250 cm^{-1}.

Transfer of the scale factor for the torsional mode ν_{10} from **1122T** to **1122G** places it in the latter at 74 cm^{-1}.

11122. There appear to be no problems associated with assignment in this molecule.

However, the B3LYP force field with the six scale factors listed in Table 10 is unable to fit ν_2 and ν_3 at 1392 and 1310 cm^{-1}, respectively, as shown in column nine of Table 7. Introduction of additional factors yielded no improvement. Instead, the satisfactory fit of column 10 was achieved by changing the off-diagonal constant between CC stretching and CH bending from 0.143 to 0.195 aJ $Å^{-1}$, before scaling. The resulting six scale factors were very close to those previously obtained.

0 and **111222**. These two molecules are included primarily to allow further exploration of the extent to which scale factors for a particular type of internal coordinate can be transferred from one symmetry species to another, within the same molecule.

Although extensive data are available for isotopomers of ethane,[54] for maximum comparability with the other molecules in this series, only the d_0 data and the value of ν^{is}CH from the d_5 isotopomer are utilized. Table 9 shows that a quite good fit is obtained with only four scale factors − νCH, δCH_3(asym and sym), ρCH_3 and the torsion. A significant improvement in the fit is only obtained when the E_u and E_g methyl rocking scale factors are allowed to differ, in the five parameter fit of column four. These scale factors are included in Table 10.

111222 behaves in a similar way, in that the largest errors are found associated with the lowest mode in the E_u and E_g classes; proportionally, these are quite significant.

However, there may be uncertainty associated with ν_{12}, for which the gas-phase value cited, 372 cm^{-1}, [55] is 10 cm^{-1} less than that in the liquid,[56] which is unusual.

Elsewhere, allowing differing factors for symmetric and antisymmetric CF stretching makes for a small improvement in the fit, as in the four parameter data shown in column seven.

These two molecules together therefore provide some evidence that scale factors for a particular type of coordinate may not be transferred within the same molecule with high precision. For the CF stretches, this might be associated with differing anharmonicities in the respective vibrations of the actual molecule.

II. Scale factors. These are collected in Table 10. Examining first those for CH stretching in part A, a fair degree of consistency can be seen among the CH type bonds, for which the average value is 0.9277. The range covered by the values for the CH^x type bonds is larger, due to the high value found in **1**, though the average is only slightly greater (0.9285) than for the CH ones. The increase from **12T** to **12G** for the CH_g bond seems to be real. However, a clear increase in scale factor occurs in the case of the CH^{xx} bonds, the average here being 0.9374. All of these values are greater than the single factor of 0.9125 for all bonds employed by Baker and Pulay,[17] which will in part reflect the triple-ζ basis set used in the present work.

Among the other types of scale factor in part B of Table 10, the differences between the present work and that of the B3PW91 survey are greater. For CF stretching, for instance, the factor is never less than unity and appears to vary by up to 5%, as in **111222**. The difference found between HCH type and HCC type factors by Baker and Pulay reoccurs to some extent in the present data, e.g., in the methyl bending motions in **0**, **11**, and **111**, but the CH_2 bending factors in the present work display either a much greater variability, as in the well determined set for **1**, or a smaller variability, as in the case of **12G**.

We agree on scale factors greater than unity for CF bending. Although most of the B3LYP/tz ones are smaller than the B3-PW91/6-31G* ones, there is one for **1112**, 1.1420, which is far above the average. It is possible that a part of these differences could stem from differences in the type of coordinate defined.

Perhaps the most striking feature of the factors listed in Table 10 is the variability of that for torsion, which ranges from a minimum of 0.8404 in **11** to a maximum of 1.4630 in **111222**.

These comparisons not only indicate the undesirability of assuming a constant factor for a given type of coordinate but also underline the danger of assuming a linear relation between scale factor and frequency, as in earlier MP2 calculations.[20,22]

III. ν^{is}CH and Correlations with CH Bond Length. The result of this survey has been to add eleven ν^{is}CH values, shown in column five in Table 1, to the six known from isotopic studies and listed in column three of this Table. Those remaining to be determined include one for the CH^x bond in **112C$_s$**, and two CH^{xx} ones, in **112C$_s$** and **1122G**. Several of the new values, in **11**, 1**2G**, and **112C$_1$**, depend on the assumption of identical scale factors for the same type of CH bond.

The extent to which these new values are compatible with those observed directly is best shown in the correlation plots of Figures 2, 3, and 4, where both kinds are plotted as "ν^{is}CH(exptl)" against the QC CH bond length determined at HF/tz, MP2/tz and B3LYP/tz levels, respectively. Data for the linear regression analyses are given in Table 11, part A, which includes the parameters obtained in the earlier study.[39]

The HF plot in Figure 2 shows very different correlations for the three kinds of bond. However, the gradients for the CH and CH^x types are very similar. The parameters for the six CH bonds are identical to those obtained earlier for four such bonds only.[39] The largest anomaly for a CH^x bond is due to the point for **12T**, which lies 5.5 cm^{-1} away from the line. This point is based on one of the more reliable ν^{is}CH values and is associated with the scale factor anomaly mentioned above. The four CH^{xx}

TABLE 11: Parameters of Regression Analyses for Correlations in Fluoroethanes

A. r_eCH(Å) = $a + b\ \nu^{is}$CH$_{expt}$(cm^{-1})

level	bond type	N^a	a	$-b \times 10^3$	$-R^b$
HF	CH	6	1.304 51(1 354)	0.073 89(4 55)	0.9925
HF[c]	CH	4	1.307(19)	0.075(7)	0.993
HF	CH^x	7	1.320 44(1 987)	0.080 32(6 70)	0.9830
HF	CH^{xx}	4	1.253 71(2 170)	0.058 20(7 26)	0.9848
MP2	CH	6	1.292 85(1 957)	0.067 48(6 57)	0.9816
MP2	CH^x	7	1.344 97(2 953)	0.085 19(9 96)	0.9675
MP2	CH^{xx}	4	1.293 42(1 689)	0.067 63(5 64)	0.9931
MP2	All	17	1.28565(1482)	0.065 10(4 98)	0.9588
MP2[c]	All	6	1.285(18)	0.065(6)	0.984
B3LYP	CH	6	1.297 49(2 021)	0.068 96(6 79)	0.9812
B3LYP[c]	CH	4	1.301(30)	0.070(10)	0.980
B3LYP	CH^x	7	1.332 41(3 408)	0.080 72(1 150)	0.9528
B3LYP	CH^{xx}	4	1.234 80(2 552)	0.047 54(8 53)	0.9693

B. r_e(Å) = $a + b\ f_{unsc}$(aJ Å^{-2})

level	bond type	N[a]	a	$-b \times 10^3$	$-R^b$
HF	CF	6	1.544 7(10 2)	0.026 7(15)	0.9938
HF	CF^x	8	1.519 9(10 0)	0.0252(14)	0.9914
HF	CF^{xx}	6	1.507 0(10 1)	0.024 6(13)	0.9946
B3LYP	CF	6	1.586 7(12 9)	0.035 5(23)	0.9916
B3LYP	CF^x	8	1.560 4(86)	0.034 0(15)	0.9943
B3LYP	CF^{xx}	6	1.541 5(72)	0.032 6(12)	0.9974
HF	CH	6	1.197 8(10 8)	0.019 7(19)	0.9823
HF	CH^x	8	1.184 5(12 3)	0.017 5(21)	0.9592
HF	CH^{xx}	6	1.180 7(17 1)	0.016 9(29)	0.9470
HF	CH(all)	20	1.198 8(52)	0.0199(9)	0.9824
B3LYP	CH	6	1.205 3(13 7)	0.021 5(26)	0.9720
B3LYP	CH^x	8	1.199 9(14 5)	0.020 5(28)	0.9487
B3LYP	CH^{xx}	6	1.201 5(16 4)	0.020 7(31)	0.9570
B3LYP	CH(all)	20	1.199 5(74)	0.020 4(14)	0.9595

C. f_{unsc}CH (aJ Å^{-2}) = $a + b\ \nu^{is}_{unsc}$CH(cm^{-1})

level	bond type	N^a	a	$b \times 10^3$	R^b
HF	CH(all)	18	−5.014(71)	3.332(22)	0.9996
B3LYP	CH	6	−4.893(52)	3.288(17)	1.0000
B3LYP	CH^x	8	−4.882(99)	3.281(32)	0.9997
B3LYP	CH^{xx}	6	−4.811(66)	3.255(21)	0.9999

[a] Number of data employed. [b] Correlation coefficient [c] Earlier result from directly observed values only.

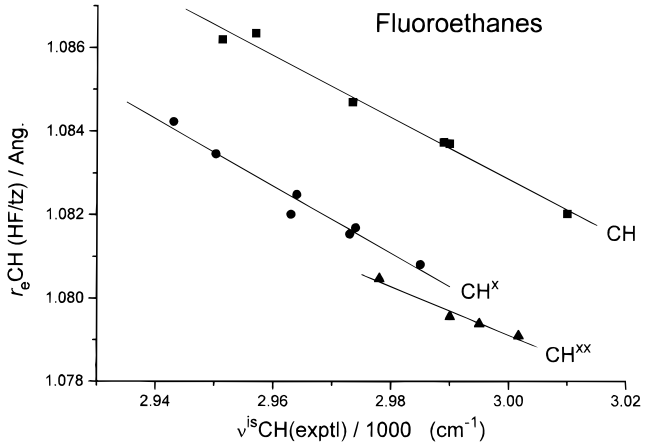

Figure 2. Correlation between r_eCH(HF/tz) and ν^{is}CH(exptl).The latter include values derived from scaling the QC force field. Parameters in Table 11, part A.

points actually lie on a shallow curve, so that the linear regression gradient may not be very significant.

The combined seventeen MP2 data in Figure 3 are fitted by a line showing some scatter, but with parameters identical to those obtained earlier, with only six data. Analysis of the separate types of bond shows a close agreement between the

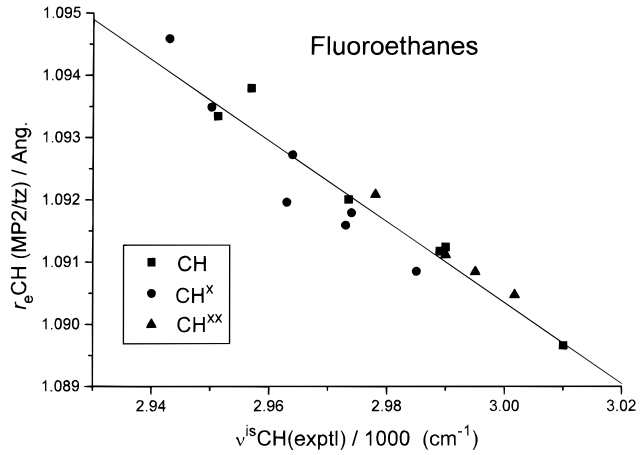

Figure 3. Correlation between r_eCH(MP2/tz) and ν^{is}CH(exptl.). Parameters in Table 11, part A.

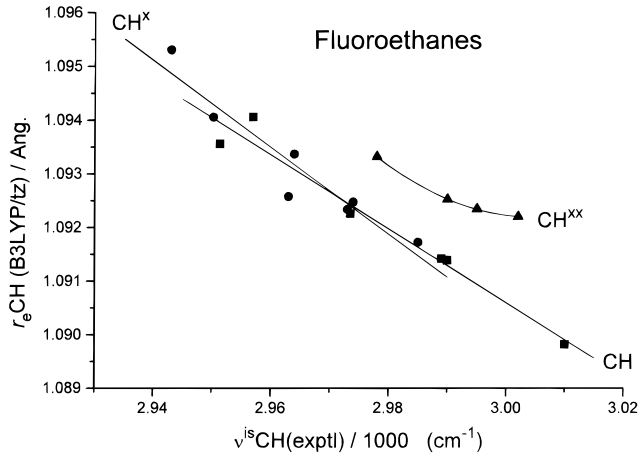

Figure 4. Correlation between r_eCH(B3LYP/tz) and ν^{is}CH(exptl.). Parameters in Table 11, part A.

TABLE 12: Predictions of ν^{Is}CH (cm^{-1}) in 112C$_s$ and 1122G

species	bond	eqn order[a]	HF/tz	MP2/tz[b]	B3LYP/tz	MP2/tz[c]
112C$_s$	CH$^x_{gt}$	1	2961	2960(2962)	2957	2964
	CH$^{xx}_t$	1	2951	2951(2946)	2931	2947
	CH$^{xx}_t$	2	2986	2974	3074	
1122G	CH$^{xx}_{gt}$	1	2986	2986(2983)	2991	2984
	CH$^{xx}_{gt}$	2	2984	2985	2979	

[a] 1 = linear, as in Table 11; 2 = quadratic. [b] In parentheses, values from combined CH, CH^x, and CH^{xx} data ("All" in Table 11). [c] From reference (39).

CH and CH^{xx} types but a distinction between these and the CH^x plot. Mild curvature can also be detected in the CH^{xx} plot, possibly also in the CH^x one.

By contrast, in the B3LYP correlations of Figure 4, the CH and CH^x types are roughly collinear, whereas the CH^{xx} one is markedly displaced and curved. Although four points are hardly adequate to define curvature, the values of ν^{is}CH involved come from apparently reliable determinations. The presence of this curvature makes it hard to make any kind of precise prediction of ν^{is}CH for the CH$^{xx}_t$ bond in **112C$_s$**, since its bond length (Table 1) is in each case well outside the range covered by the four determined values.

Table 12 shows the predictions of ν^{is}CH for all three of the undetermined cases, obtained either from the correlation for the particular bond type, or in the case of the MP2 correlations, from the overall fit to all seventeen data as well. Very little change from the earlier estimates is indicated for either the CH$^x_{gt}$ bond in **112C$_s$** or the CH$^{xx}_{gt}$ one in **1122G**. For the latter, the

TABLE 15: Computed Unscaled *ν*CH/*ν*CH Interaction Force Constants (aJ Å^{-2})

	f'_α (gem)			f'_β (vicinal)			
species	atoms[a]	HF	B3LYP	atoms[a]	type[b]	HF	B3LYP
0[c]	H, H	0.0602	0.0507		*g*	0.0146	0.0103
					t	−0.0162	−0.0177
1[d]	H_a, H_a	0.0515	0.0440	H_s, H^x	*g*	0.0148	0.0108
	H_a, H_s	0.0479	0.0396	H_a, H^x	*g*	0.0142	0.0103
	H^x, H^x	0.0737	0.0651	H_a, H^x	*t*	−0.0147	−0.0157
11	H_a, H_a	0.0427	0.0361	H_a, H^x	*g*	0.0139	0.0101
	H_a, H_s	0.0397	0.0335	H_s, H^x	*t*	−0.0126	−0.0130
12T		0.0626	0.0552		*g*	0.0133	0.0093
					t	−0.0116	−0.0122
12G		0.0593	0.0516	$H^x{}_s$, $H^x{}_t$	*g*	0.0118	0.0083
				$H^x{}_t$, $H^x{}_t$	*g*	0.0191	0.0153
				$H^x{}_s$, $H^x{}_g$	*t*	−0.0108	−0.0104
111		0.0363	0.0321			-	-
112C$_s$		0.0561	0.0501	$H^{xx}{}_s$, $H^x{}_{gt}$	*g*	0.0152	0.0119
112C$_1$		0.0505	0.0445	$H^{xx}{}_s$, $H^x{}_{gt}$	*g*	0.0123	0.0089
				$H^{xx}{}_s$, $H^x{}_{gg}$	*t*	−0.0082	−0.0076
1112		0.0484	0 0447			-	-
1122T		-	-		*t*	−0.0045	−0.0033
1122G		-	-		*g*	0.0135	0.0104
Average					*g*	0.0143	0.0109
Average					*t*	−0.0112	−0.0114

[a] Terminal atoms of the two CH bonds concerned, where ambiguity exists. H_s, H_a are atoms in and out of the symmetry plane respectively, in **1** and **11**. [b] *g, t* indicate gauche and trans interactions, respectively. [c] Values from an empirical general force field: f'_α; 0.037, f'_β; 0.002(g), −0.013(t).[54] [d] Values from a form of local mode treatment: f'_α; 0.037(H_a, H_a), 0.031(H_a, H_s) 0.058(H^x, H^x): f'_β; 0.014(g, H_s, H^x), 0.014(g, H_a, H^x), −0.012(t, H_a, H^x).[47]

assumption of a linear or quadratic fit has virtually no effect on the value from the HF and MP2 plots, but a larger one from the B3LYP correlation. For the $CH^{xx}{}_t$ bond in **112C$_s$** however, the presence or absence of curvature makes a difference that is large at the HF and MP2 levels and improbably large in the B3LYP case.The extrapolation distance involved is clearly far too great. However, there is at least the possibility here that ν^{is}CH for **112C$_s$** may be somewhat larger than the low value of 2947 cm^{-1} presupposed in the discussion of the *ν*CH region of the spectrum above. This would then entail a scale factor greater than that for the corresponding bond in **112C$_1$**, as postulated above as an alternative to a large upward frequency shift upon condensation.

IV. **Valence Stretching Force Constants, Bond Lengths and Offset Values.** Unscaled valence force constants *f* and bond length r_e data derived from HF/tz and B3LYP/tz treatments are included in Tables 1, 13S, and 14S for the CH, CF, and CC bonds. Tables 15, 16S, 17S, and 18S contain values of interaction force constants *f* ′ for the stretches involving CH/CH, CF/CF, CH/CF, CC/CH, and CC/CF, respectively.

CF Bond and Offset Values. Regression analysis data for the plots of r_eCF versus *f*CF at the two levels of theory employed are given in part B of Table 11. Excellent linear correlations result for a given type of bond, CF, CF^x, or CF^{xx} but each is markedly displaced from the others. Clearly, the QC calculation is producing a different type of potential energy curve for each of the three types of CF bond. A very similar distinction in behavior between the three types of bond is seen in correlations between r_eCF and the Mulliken charge on fluorine.[63] The postulated change in the potential surface suggests that a variation in 'offset' value associated with r_eCF may be occurring.

The term "offset" owes its origin to the earlier explorations of the structures of organic compounds by the ab initio method, at the Hartree−Fock level and with modest basis sets, where systematic differences in bond lengths between those determined ab initio and experimental values were found. [25,60−62]

Evidence that such offset values may not in fact be constant was obtained in the recent work on fluoro-and chloroethanes.[39]

TABLE 19: Average Offset Values $r_e - r_a$ for CF Bonds in Fluoroethanes[a]

bond type	HF/tz	MP2/tz	B3LYP/tz
CF	−0.028 2(55)	−0.008 4(48)	−0.000 6(60)
CF^x	−0.018 3(31)	0.003 9(32)	0.010 6(38)
CF^{xx}	−0.017 8(27)	0.005 8(33)	0.012 2(36)

[a] r_e and r_a values from this work and reference (39).

In the case of the CF bond, a linear correlation between r_e(QC) and r_a derived from a consistent set of electron diffraction studies for all the fluoroethanes, had a gradient at all levels of theory substantially less than 1.0. If the individual offset values $r_a - r_e$(true) and r_e(QC) − r_e(true) were both constant, the gradient should be unity. In the absence of any obvious reason why the r_a offset value should be varying, the suspicion fell on that for r_e(QC).

The displaced lines of Table 11B suggest a possible explanation for the low gradient of the r_e(QC) versus r_a correlation. The variation in either r_e or r_a is associated with a progressive shortening of the bond due to increasing numbers of fluorine atoms. The overall gradient may then be influenced by the presence of different scale factors for the different types of CF bond. Table 19 shows the average values of the offset value r_e(QC) − r_a calculated using the r_a values cited in reference (39) and the r_e values at the HF, MP2, and B3LYP levels from the latter and from this work. Despite large standard deviations, which seem likely to stem largely from the approximations inherent in the electron diffraction experiment, such as identical bond lengths for two conformers, there does appear to be a trend toward a more positive offset value in all three calculations.

A similar study for the SiCl bond was caried out in a series of conformations of disilylamines $NR(SiHMeCl)_2$ (R═H, Me). The very close correlation ($R = 0.9994$) between r_e and *f*, both calculated at the HF/6-31G* level, obviously reflects the single type of group, SiHMeCl, involved.[40]

CH Bond and Offset Values. A close link between r_eCH and *f*CH is of course implicit in the correlations already provided

between r_eCH and ν^{is}CH(exptl) in Figures 2−4. However, it is pertinent to enquire whether the irregularities in these plots, which are absent in similar ones for hydrocarbons,[36−38] are due either to changes in the form of the potential energy curve, as apparently occurs for the CF bond, or more simply to a breakdown in the assumption of "isolation" in the normal modes for which ν^{is}CH is calculated.

Regression data for plots of r_eCH versus *f*CH(unscaled) are included in part B of Table 11, for both the HF and B3LYP calculations. For a particular type of CH bond, the scatter is markedly greater than that for the CF bond, but the displacements of the correlation lines from each other are much smaller and probably not significant.

The query concerning "isolation" may be answered by plotting *f*CH against the unscaled ν^{is}CH value, the data for which are contained in part C of Table 11. With the HF based data, the one-to-one relationship is impeccable for all bonds. With the B3LYP data, there are small displacements amounting to about 3 cm^{-1} between the CH and CH^x lines and 2 cm^{-1} between the CH^x and CH^{xx} ones. These displacements mean that the likely effect on ν^{is}CH of a variation in the degree of isolation of the CH mode, from a methyl group through to methylene and methine, is insignificant, and certainly much less than the changes exhibited in the plots of Figures 2-4, which involve "experimental" ν^{is}CH values.

Similar QC studies of the SiH bond were carried out in connection with the work described in reference (39). For fluoro- and chlorodisilanes up to trisubstitution,(**111** and **112**) correlations between ν^{is}SiH(unscaled) and r_eSiH involved substantially less scatter, with correlation coefficients of 0.9957(F, HF/6-31G*), 0.9829(F, MP2/6-31G*), and 0.9961(Cl, HF/6-31G*), and with no discrimination visible between SiH, SiH^x, and SiH^{xx} bonds.

It therefore appears that the presence of fluorine adjacent to a CH bond leads to small specific and unpredictable variations in the QC treatments of a series such as the fluoroethanes, at the levels employed here, which are absent for SiH bonds.

In seeking evidence for the constancy or otherwise of offset values for the CH bond length, the problem lies in finding experimental bond lengths of adequate precision. The effects of zero point energy on rotational constants necessitate the introduction of isotopic changes in the different types of average bond length determined and no such studies have yet been made in the fluoroethanes. The absence of a fluorine isotope is a further handicap. Although there are as yet no r_z, let alone experimental r_e structures, for any fluoroethanes, the existence of a correlation between experimental r_eCH values in other compounds and ν^{is}CH is of great value.[34] The gradient of the latter, $-7.18(17) \times 10^{-5}$, is substantially less than that of the earlier correlation[33] involving r_0, -10.23×10^{-5}, which implies that the offset value for r_0 is varying.

Examining the gradients in Table 11A, it is seen that most have values agreeing with -7.18×10^{-5} within the errors involved, so that in these cases, there is no evidence for r_e(QC) offset variation *within each sequence*. In fact, significant deviations occur only for the CH^{xx} bond at the HF and B3LYP levels. However, the displacements of the correlations from each other, which is also a feature of the HF and B3LYP diagrams, implies offset variation among the three types of bond, CH, CH^x, and CH^{xx}, as it does for CF bonds.

A more localized symptom of offset variation is likely to be the change in CH stretching scale factor evident from **12T** to **12G**, to which it may be necessary to add similar changes from **112C$_1$** to **112C$_s$** and **1122T** to **1122G**.

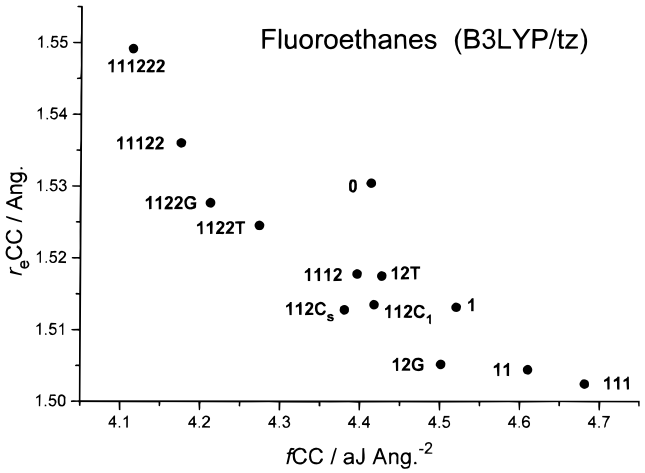

Figure 5. Scatter diagram, r_eCC(B3LYP/tz) versus *f*CC(B3LYP/tz, unscaled).

CC Bonds. Figure 5, displaying B3LYP/tz data, shows a rough connection between valence force constant and bond length, which, if the high point for ethane itself is ignored, might justify a curve. There is a notable difference between the points for the two **12** conformers.

The similar plot for HF/tz data, not shown, appeared to give a random distribution.

Interaction Constants f′. An inspection of Tables 15−18S shows that these are all positive, except for those involving two kinds of trans-related pairs of bonds, CH/CH and CH/CF. For these pairs of bonds, trans constants f'_t are always negative at the B3LYP level and either negative or very small at the HF one. With $f'_{CH/CH}$, quite good agreement is found (Table 15) between the HF and B3LYP values of these data, the latter being always slightly less than the former. This agreement accounts for the similar ν^{is}CH values derived above by each approach from the same observed frequencies of the parent molecule. The trends in both f'_α and f'_β in **1** agree well with those found in an earlier energy factored force field analyses of observed νCH data, as shown in Table 15, footnote *d*. Assignments in the νCH region which implicitly contravene these trends are suspect.

As might be expected, *f′* values are somewhat larger for pairs of CF bonds (Table 16S), f'_α occurring in the range 0.85−0.94 (HF) or 0.79−0.86(B3LYP) aJ $Å^{-2}$. From the B3LYP calculation, the average f'_β values are 0.071 aJ $Å^{-2}$ (trans) and 0.089 aJ $Å^{-2}$ (gauche), so that the pronounced conformational difference for CH bonds is present here also to a small degree. However, HF/tz data for CF bonds do not show this difference.

f'_α for CH/CF pairs (Table 17S) falls in the range 0.22−0.25(HF) or 0.21−0.24(B3LYP) aJ $Å^{-2}$. The corresponding values of f'_β vary from 0.02 to 0.04 (HF) or 0.01 to 0.03(B3LYP) aJ $Å^{-2}$ for gauche related bonds and average 0.006 (HF) or −.003(B3LYP) aJ $Å^{-2}$ for the trans pairs.

Both CH/CC and CF/CC f'_α interactions (Table 18S) differ from the previous types in that the B3LYP values are slightly greater than the HF ones. The CH/CC interaction can vary markedly within the same moleule, for example, 0.093(CH^x), 0.065(CH_{gg}), 0.042(CH_{gt}) aJ $Å^{-2}$ in **11** (B3LYP values). The corresponding quantities for the CF/CC interaction in the analogous molecule **1112** are 0.293(CF_{ggt}), 0.298($CF^{xx}{}_t$), and 0.302($CF^{xx}{}_g$) aJ $Å^{-2}$.

V. General Discussion. Three general matters are raised by this work:

(1) The need for further experimental work, particularly using jet-cooled gas phase and argon matrix trapped infared spectra,

has been already emphasized. However, additional features of existing spectra that merit attention are the large changes of frequency evident from gas to crystal which appear to characterize both νCH and νCF modes. The former rise, whereas the latter tend to fall. Exploration of the intermolecular forces involved in both situations would be profitable, as well as helpful for clearing up problems in assignment.

(2) A second matter concerns methodology. Are valence stretching force constants the best type of quantity for an exploration of the relationships between equilibrium properties such as the bond length and dynamical properties of the bond? In recent work by Cremer and co-workers, alternative quantities, the adiabatic internal mode, and its associated adiabatic stretching force constant and frequency have been proposed, which appear to have many advantages.[64,65] These include the avoidance of any concern about the degree of isolation assocated with ν^{is}CH. It would be interesting to see if these adiabatic quantities exhibit the same irregularities of behavior in the QC derived information for the fluoroethanes as is evident in the present work.

(3) The third question is the extent to which the preliminary conclusions made here may be affected by anharmonicity. The extent to which this is present is considerable in νCH motions, perhaps 4−5%,[66] and appreciable for νCF ones, where an estimate in CH_3F is about 2.7%.[67]

The issue is whether anharmonicity is varying along a series of compounds such as the fluoroethanes. The likelihood of such variations in CH anharmonicity affecting conclusons based on ν^{is}CH was discussed recently and considered to be negligible, on the basis of admittedly limited evidence.[39] Whether νCF anharmonicity varies in this respect is as yet unknown. The need for QC calculations of anharmonic force fields is clearly strong.

Appendix

Symmetry coordinates were based on internal coordinates differing from those of reference (25) in the following instances: (a) bond stretches: appropriate combinations from symmetrically equivalent bonds only. (b) CH_3 and CF_3 groups: symmetric deformations, $\delta_s CH_3 = \Sigma H_i CH_j$, $\delta_s CF_3 = \Sigma F_i CF_j$. (c) CH_2F group: CH_2 scissors, $\delta_s CH_2 = H_i CH_j$; CF bend = FCC. (d) CHF_2 group: CF_2 scissors, $\delta_s CF_2 = F_i CF_j$; CF_2 twist, $\tau CF_2 = F_i CC - F_j CC$.

With these coordinates, there were occasionally large off-diagonal terms in the potential energy distribution (PED). The same coordinate might produce such terms in one symmetry species but not in another. Trials with coordinates of the type recommended in reference (25) showed no improvement in this respect.

A general feature of the PEDs was the high proportion of CF bending in modes above 1000 cm^{-1} conventionally described as composed of CF stretching and/or CH bending motions.

Acknowledgment. I thank Dr Carole Morrison for valuable assistance in the use of the Gaussian 94 program, the EPSRC for the Edinburgh ab initio facility, funded by Grant No. GR/K/04194, and a reviewer for a careful reading of the MS and helpful comment.

Supporting Information Available: Unscaled valence force constants and bond lengths for CH and CF bonds (Table 13S), and CC bonds (Table 14S): stretch−stretch force constants for the interactions CF/CF (Table 16S), CH/CF (Table 17S), CH/CC and CF/CC (Table 18S); 6 pages.

References and Notes

(1) Saur, O.; Travert, J.; Saussey, J.; Lavalley, J.-C. *J. Chim. Phys.* **1975**, *72*, 907.
(2) Huber-Wälchli, P.; Günthard, Hs. H. *Chem. Phys. Lett.* **1975**, *30*, 347.
(3) Bürger, H.; Niepel, H.; Pawelke, G. *Spectrochim. Acta* **1980**, *36A*, 7.
(4) Harris, W. C.; Holtzclaw, J. R.; Kalasinsky, V. F. *J. Chem. Phys*. **1977**, *67*, 3330.
(5) Kalasinsky, V. F.; Anjaria, H. V.; Little, T. S. *J. Phys. Chem*. **1982**, *86*, 1351.
(6) Fraser, G. T.; Pine, A. J.; Domeneck, J. L.; Pate, B. H. *J. Chem. Phys*. **1993**, *99*, 2396.
(7) McNaughton, D.; Evans, C.; Robertson, E. G. *J. Chem. Soc., Faraday Trans*. **1995**, *91*, 1723.
(8) McNaughton, D.; Evans, C. *J. Phys. Chem*. **1996**, *100*, 8660.
(9) Hansford, G. M.; Davies, P. B. *J. Mol. Spectrosc*. **1996**, *180*, 345.
(10) Nakanaga, T.; Ito, F.; Miyawaki, J.; Sugawara, K.; Takeo, H.; Suga, A. *J. Mol. Spectrosc*. **1996**, *178*, 40.
(11) Stone, S. C.; Philips, L. A.; Fraser, G. T.; Lovas, F. J.; Xu, L.-H.; Sharpe, S. W. *J. Mol. Spectrosc*. **1998**, *192*, 75.
(12) Speis, M.; Buss, V. *J. Comput. Chem*. 1992, *13*, 142.
(13) Chen, Y.; Paddison, S. J.; Tschuikow-Roux, E. *J. Phys. Chem*. **1994**, *98*, 1100.
(14) Papasavva, S.; Illinger, K. H.; Kenny, J. E. *J. Phys. Chem*. **1996**, *100*, 10 100.
(15) Tai, S.; Illinger, K. H.; Papasavva, S. *J. Phys. Chem*. A **1997**, *101*, 9749.
(16) Parra, R. D.; Zeng, X. C. *J. Phys. Chem*. A **1998**, *102*, 654.
(17) Baker, J.; Pulay. P. *J. Comput. Chem*. **1998**, *19*, 1187.
(18) Chen, K.-H.; Walker, G. A.; Allinger, N. L. *J. Mol. Struct*. **1999**, *490*, 87.
(19) Durig, J. R.; Liu, J.; Little, T. S.; Kalasinsky, V. F. *J. Phys. Chem*. **1992**, *96*, 8224.
(20) Papasavva, S.; Tai, S.; Esslinger, A.; Illinger, K. H.; Kenny, J. E. *J. Phys. Chem*. **1995**, *99*, 3438.
(21) Eltayeb, S.; Guirgis, G. A.; Fanning, A. R.; Durig, J. R. *J. Raman Spectrosc*. **1996**, *27*, 111.
(22) Tai, S.; Papasavva, S.; Kenny, J. E.; Gilbert, B. D.; Janni, J. A.; Steinfeld, J. I.; Taylor, J. D.; Weinstein, R. D. *Spectrochim. Acta* **1999**, *55A*, 9.
(23) McKean, D. C. *Chem. Soc. Rev*. **1978**, *7*, 399.
(24) McKean, D. C.; Saur, O.; Travert, J.; Lavalley, J.-C. *Spectrochim. Acta* **1975**, *31A*, 1713.
(25) Pulay. P.; Fogarasi, G.; Pang. F.; Boggs, J. E. *J. Am Chem. Soc*. **1979**. *101*, 2554.
(26) Gough, K. M.; Murphy, W. F.; Raghavachari, K. *J. Chem. Phys*. **1987**, *87*, 3332.
(27) McKean, D. C.; McQuillan, G. P.; Murphy, W. F.; Zerbetto, F. *J. Phys. Chem*. **1990**, *94*, 4820.
(28) Murphy, W, F.; Zerbetto, F.; Duncan, J. L.; McKean, D. C. *J. Phys. Chem*. **1993**, *97*, 581.
(29) McKean, D. C.; McQuillan, G. P.; Murphy, W, F.; Mastryukov, V. S.; Boggs, J. E. *J. Phys. Chem*. **1995**, *99*, 8994.
(30) McKean, D. C.; McPhail, A. L.; Edwards, H. G. M.; Lewis, I. R.; Murphy, W. F.; Mastryukov, V. S.; Boggs, J. E. *Spectrochim. Acta* **1995**, *51A*, 215.
(31) McKean, D. C.; Edwards, H. G. M.; Lewis, I. R.; Murphy, W. F.; Mastryukov, V. S., Boggs, J. E.*Spectrochim. Acta* **1995**, *51A*, 2237.
(32) McKean, D. C. *Spectrochim. Acta* **1999**, *55A*, 1485.
(33) McKean, D. C.*J. Mol. Struct.* **1984**, *113*, 251.
(34) Demaison, J. Wlodarczak, G. *Struct. Chem*. **1994**, *5*, 57.
(35) Henry, B. R. *Acc. Chem. Res*. **1987**, *20*, 429.
(36) Snyder, R. G.; Aljibury, A. L.; Strauss, H. L.; Casal, H. L.; Gough, K. M.; Murphy, W. F. *J. Chem. Phys*. **1984**, *81*, 5352.
(37) Aljibury, A. L.; Snyder, R. G.; Strauss, H. L.; Raghavachari, K. *J. Chem. Phys*. **1986**, *84*, 6874.
(38) Schäfer, L.; Siam, K. *J. Chem. Phys*. **1988**, *88*, 7255.
(39) Fodi, B.; McKean, D. C.; Palmer, M. H. J. *Mol. Struct*. **2000**, *500*, 195.
(40) Fleischer, H.; McKean, D. C.; Pulham, C. R.; Bühl, M. *J. Chem. Soc., Dalton* Trans. **1998**, 585.
(41) Rauhut, G.; Pulay, P. *J. Phys. Chem*. **1995**, *99*, 3093.
(42) Gaussian 94 (Revision C2); Frisch, M. J.; Trucks, G. W.; Schlegel, H. B.; Gill, P. M. W.; Johnson, B. G.; Robb, M. A.; Cheeseman, J. R.; Keith, T. A.; Petersson, G. A.; Montgomery, J. A.; Raghavachari, K.; Al-Laham, M. A.; Zakrzewski, V. G.; Ortiz, J. V.; Foresman, J. B.; Cioslowski, C.; Stefanov, B. B.; Nanayakkara, A.; Challacombe, M.; Peng, C. Y.; Ayala, P. Y.; Chen, W.; Wong, M. W.; Andres, J. L.; Replogle, E. S.; Gomperts, R.; Martin, R. L.; Fox, D. J.; Binkley, J. S.; Defrees, D. J.; Baker, J.;. Stewart, J. P.; Head-Gordon, M.; Gonzalez, C.; Pople, J. A. *Gaussian Inc.:* Pittsburgh, PA, 1995.

(43) Lee, C.; Yang, W.; Parr, R. G. *Phys. Rev.* **1988**, *B37*, 785.
(44) Michlich, B.; Savin, A.; Stoll, H.; Preuss, H. *Chem. Phys. Lett.* **1989**, *157*, 200.
(45) Becke, A. D. *J. Chem. Phys.* **1993**, *98*, 5648.
(46) Hedberg, L.; Mills, I. M. *J. Mol. Spectrosc.* **1993**, *160*, 117, *Mol. Phys*., to be published.
(47) McKean, D. C.; Lavalley, J.-C.; Saur, O.; Travert, J. *Spectrochim. Acta* **1977**, *33A*, 865.
(48) McKean, D. C., unpublished work.
(49) Felder, P.; Günthard, Hs. H. *J. Mol. Spectrosc*. **1982**, *95*, 68.
(50) Felder, P.; Günthard, Hs. H. *Chem. Phys*. **1982**, *71*, 9. Felder, P.; Günthard, Hs. H. *Chem. Phys*. **1984**, *85*, 1.
(51) Beagley, B.; Brown, D. E. *J. Mol. Struct*. **1979**, *54*, 175.
(52) Brown, D. E.; Beagley, B. *J. Mol. Struct*. **1977**, *38*, 167.
(53) Mackenzie, M. W. *Spectrochim. Acta* **1984**, *40A*, 279.
(54) Duncan, J. L.; Kelly, R. A.; Nivellini, G. D.; Tullini, F. *J. Mol. Spectrosc*. **1983**, *98*, 87.
(55) Nielsen, J. R.; Gulliksen, G. W. *J. Chem. Phys*. **1953**, *21*, 1416.
(56) Rank, D. H.; Pace, E. L. *J. Chem. Phys*. **1947**, *15*, 39.
(57) Eggers, D. F.; Lord, R. C.; Wickstron, G. W. *J. Mol. Spectrosc*. **1976**, *59*, 63.
(58) Nielsen, J. R.; Richards, C. M.; McMurry, H. F. *J. Chem. Phys*. **1948**, *16*, 67.
(59) Mann, D. E.; Plyler, E. K. *J. Chem. Phys*. **1953**, *21*, 1116.
(60) Blom, C. E.; Altona, C. *Mol. Phys*. **1976**, *31*, 1377.
(61) Schäfer, L.; Van Alsenoy, C.; Scarsdale, J. N. *J. Mol. Struct*. **1982**, *86*, 349.
(62) Fogarasi, G.; Pulay, P. *Vibrational Spectra and Structure*; Durig, J. R., Ed.; Elsevier: Amsterdam, 1985; Vol. 14, p 125.
(63) Palmer, M. H. *J. Mol. Struct*. **2000**, *500*, 225.
(64) (a) Konkoli, Z.; Cremer, D. *Int. J. Quantum Chem*. **1998**, *67*, 1. (b) Konkoli, Z.; Larsson, J. A.; Cremer, D. *Int. J. Quantum Chem*. **1998**, *67*, 11. (c) Konkoli, Z.; Cremer, D. *Int. J. Quantum Chem*. **1998**, *67*, 29. (d) Konkoli, Z.; Larsson, J. A.; Cremer, D. *Int. J. Quantum Chem*. **1998**, *67*, 41.
(65) Cremer, D.; Larsdon, J. A.; Kraka, E. *Theoretical Organic Chemistry*; Párkányi, C., Ed.; Elsevier Science: Amsterdam, Vol 5, 1998, 259.
(66) Duncan, J. L. *Spectrochim. Acta* **1991**, *47A*, 1.
(67) Law, M. M.; Duncan, J. L.; Mills, I. M. *J. Mol. Struct*. **1992**, *260*, 327.